Chapter 8

Applying CJK(L) parametrizations: the $\gamma\gamma \to h/\bar{h} + X$ example

In the previous sections we have discussed the theoretical basis and the phenomenological results of the CJK(L) parton parametrizations for the photon. These parametrizations utilize the new ACOT(χ) scheme for the heavy-quark contributions to $F_2^\gamma(x, Q^2)$ and have been obtained through a serious of fits to the $\text{DIS}_{e\gamma}$ data. The resulting parton distributions as well as the photon structure function have been parametrized. Now we apply the ACOT(χ) type distributions in other than $\text{DIS}_{e\gamma}$ processes involving heavy quarks. We will consider the problem of the proper treatment of the heavy-quark kinematic thresholds in the heavy-quark production $\gamma\gamma \to h/\bar{h} + X$ experimentally observed in the e^+e^- collisions. As we discussed in Chapter 4 the disagreement between the theoretically predicted and experimentally measured values of the photon-photon beauty-quark production cross-section is a great puzzle, see [12–14]. By so far all of the calculations, using not only the DGLAP based photon parametrizations, see [77], but performed also in the CCFM [75,76] approach, predict the cross-sections lying significantly below the experimental results. The measurements and theoretical calculations differ by 2-3. Here we want to examine whether this problem is related to the description of the heavy-quark densities in the photon. In high energy e^+e^- collisions the hadronic final state is predominantly produced in $\gamma^\star\gamma^\star$ interactions, where the virtual photons are almost on mass shell. Similarly to the $\text{DIS}_{e\gamma}$ scattering case, where one of the interacting photons is quasi-real, see Chapter 3, the $e^+e^- \to e^+e^- + h/\bar{h} + X$ scattering can be effectively described with the interaction of real photons with energy spectra given by the Weizsäcker-Williams (WW) approximation [42]. The formula for the WW spectrum, $f_{\gamma/e}(z = E_\gamma/E_{\text{beam}})$ with E_{beam} being the energy of the electron beam, has been already presented in Eq. (3.9).

Heavy quarks can be produced in $\gamma\gamma$ collisions through three mechanisms. Direct (DD) production occurs when both photons couple directly to the heavy quarks in the same way as in the so-called Bethe-Heitler process, see Fig. 2.5. In a single resolved-photon processes (DR) one of photons interacts via its partons with the second photon. When both photons split into a flux of quarks and gluons, the process is labeled a double resolved photon (RR) process.

Cross-sections contributing to each of the mechanisms read

$$\begin{aligned}
\sigma(e^+e^- \to e^+e^- + h/\bar{h} + X)|_{\rm DD} &= \int_0^1 dz_a \int_0^1 dz_b \; f_{\gamma/e}(z_a) f_{\gamma/e}(z_b) \; \hat{\sigma}(\gamma\gamma \to h\bar{h}), \qquad (8.1)\\
\sigma(e^+e^- \to e^+e^- + h/\bar{h} + X)|_{\rm DR} &= 2 \int_0^1 dz_a \int_0^1 dz_b \; f_{\gamma/e}(z_a) f_{\gamma/e}(z_b) \\
&\quad \int_0^1 dx_b \; f_i^\gamma(x_b, \mu^2) \; \hat{\sigma}(\gamma i \to h/\bar{h} + X),\\
\sigma(e^+e^- \to e^+e^- + h/\bar{h} + X)|_{\rm RR} &= \int_0^1 dz_a \int_0^1 dz_b \; f_{\gamma/e}(z_a) f_{\gamma/e}(z_b) \\
&\quad \int_0^1 dx_a \int_0^1 dx_b \; f_i^\gamma(x_a, \mu^2) f_j^\gamma(x_b, \mu^2) \; \hat{\sigma}(ij \to h/\bar{h} + X),
\end{aligned}$$

where by a and b we denote two scattering photons, $f_i^\gamma(x, \mu^2)$ generally refer to the parton distributions in γ: q_i^γ, q_h^γ and G^γ and μ^2 is the hard scale of the process.

The number of the corresponding parton processes differs in the FFNS scheme and the VFNS approaches, such as ZVFNS or ACOT(χ) schemes. In the former only the reactions in which a heavy quark is created may appear, and the number of active quarks $N_f = 3$. VFNS schemes consider apart from the gluons and u, d and s quarks also heavy quarks as active, hence the list of the allowed parton processes is longer in that case. In the standard ZVFNS approach N_f varies from 3 to 5 depending on the value of the hard (factorization, renormalization) scale μ. The charm- and beauty-quarks are included in the computation provided that $\mu > m_c$ (m_b). In the ACOT(χ) scheme the number of active quarks is constant and equal to 5. All the parton reactions in the schemes of both types, contributing in the LO calculation to a heavy-quark h production, are shown in Table 8.1.

In the massive FFNS scheme we calculate parton cross-sections keeping all mass terms. On contrary in the massless ZVFNS we neglect the heavy-quark mass throughout the calculation. In the ACOT(χ) approach the processes which are common with the FFNS scheme are treated as in the massive scheme. Considering the remaining processes, in which heavy quark appears in the initial state, we have to decide how to describe them. On the one hand the ACOT(χ) scheme leads to the massless heavy-quark densities, since we apply massless DGLAP equations. On the

	DD	DR	RR
FFNS	$\gamma + \gamma \to h + \bar{h}$	$G^\gamma + \gamma \to h + \bar{h}$	$G^\gamma + G^\gamma \to h + \bar{h}$ $q^\gamma + \bar{q}^\gamma \to h + \bar{h}$
VFNS	$\gamma + \gamma \to h + \bar{h}$	$G^\gamma + \gamma \to h + \bar{h}$ $h^\gamma(\bar{h}^\gamma) + \gamma \to h^\gamma(\bar{h}^\gamma) + G^\gamma$	$G^\gamma + G^\gamma \to h + \bar{h}$ $q^\gamma + \bar{q}^\gamma \to h + \bar{h}$ $h^\gamma + \bar{h}^\gamma \to h + \bar{h}$ $h^\gamma + h^\gamma(\bar{h}^\gamma + \bar{h}^\gamma) \to h + h(\bar{h} + \bar{h})$ $h^\gamma(\bar{h}^\gamma) + q^\gamma(\bar{q}^\gamma) \to h(\bar{h}) + q(\bar{q})$ $h^\gamma(\bar{h}^\gamma) + G^\gamma \to h(\bar{h}) + G$

Table 8.1: Parton reactions contributing to the heavy-quark production in $\gamma\gamma$ collision in the FFNS and VFNS (such as ZVFNS or ACOT(χ)) schemes.

other hand, those distributions fulfill the threshold condition $q_h^\gamma = 0$ for $W \leq 2m_h$. Therefore, we will consider two possibilities of the calculation of the parton process with the heavy quarks in the initial state: one with the massless and other with the massive phase-space and invariant parton amplitudes (see Appendix B), denoting them the 'massless' and 'massive' version of the ACOT(χ) scheme, respectively.

As discussed in detail in Section 4.3, in order to improve the description of the heavy-quark threshold in the DIS process, one introduces in the ACOT(χ) scheme the χ_h variables:

$$\chi_h = x(1 + \frac{4m_h^2}{Q^2}), \tag{8.2}$$

and calculates the heavy-quark contribution to the photon structure function as

$$\begin{aligned} F_{2,h}^\gamma|_{\mathrm{ACOT}}(x, Q^2, m_h^2) &= x e_h^2 (q_h^\gamma + \bar{q}_h^\gamma)(\chi_h, Q^2) + F_{2,h}^\gamma(x, Q^2)|_{\mathrm{res}} + F_{2,h}^\gamma(x, Q^2)|_{\mathrm{dir}} \\ &- F_{2,h}^\gamma(\chi_h, Q^2, m_h^2)|_{\mathrm{dir,sub}} - F_{2,h}^\gamma(\chi_h, Q^2, m_h^2)|_{\mathrm{res,sub}} \end{aligned} \tag{8.3}$$

(where we have repeated Eq. (4.35)). In all our analyses, the heavy-quark densities have been further parametrized as functions of x and Q^2. That means, that for a given x value parametrization returns the final density $q_h(x, Q^2)$ which should be understood as being equivalent to $q_h(\chi_h(x, Q^2), Q^2)$ with $\chi_h(x, Q^2)$ given by expression (8.2).

In the case of other resolved-photon processes involving heavy quarks we should use $q_h^\gamma(\chi_h(x, \mu^2), \mu^2)$, where μ^2 is the hard scale of given process. Such procedure is a simple analogy to the $q_i^\gamma(x, Q^2) \to q_i^\gamma(x, \mu^2)$ replacement applied for the light-quark densities. In the $\gamma\gamma \to h/\bar{h} + X$ production case one usually chooses $\mu = p_T$, the transverse momentum of the produced heavy quark (or its so-called transverse mass, $E_T = \sqrt{p_T^2 + m_h^2}$). There appears a crucial question: should now the χ_h variable be indeed defined in the same way as in the DIS$_{e\gamma}$ case? A trivial exchange of Q^2 with p_T^2 leads for a given x to the $q_h^\gamma(\chi_h, p_T^2)$ density with

$$\chi_h = x(1 + \frac{4m_h^2}{p_T^2}). \tag{8.4}$$

As can be easily shown such a choice does not fulfill the $\chi_h \to 1$ for $W \to 2m_h$ condition, necessary for a correct description of the heavy-quark threshold. The reason is that unlike in the DIS$_{e\gamma}$ process, where the invariant mass of the $\gamma^*\gamma$ system is $W^2 = Q^2(1-x)/x$, the corresponding invariant mass in the $\gamma\gamma$ cross-section is $W^2 = z_a z_b s$, with $s = 4E_{\mathrm{beam}}^2$. As in that case there is no direct relation between W and p_T, the transverse momentum can be zero and still charm- or beauty-quark distribution may appear. Moreover, formula (8.4) leads to nonzero $q_h^\gamma(\chi, p_T^2)$ under the condition

$$p_T^2 > \frac{x}{1-x} 4m_h^2, \tag{8.5}$$

which for instance for $x = 0.6$ gives $p_T^2 > 6m_h^2$. Typical condition adopted in many works is $p_T^2 > m_h^2$, which also has no relation with the real threshold condition $W > 2m_h$.

The solution of the above problem is straightforward. The χ_h variable given by formula (8.2) can be rewritten in the form exposing dependence on W, namely

$$\chi_h = x + \frac{4m_h^2}{W^2}(1-x), \tag{8.6}$$

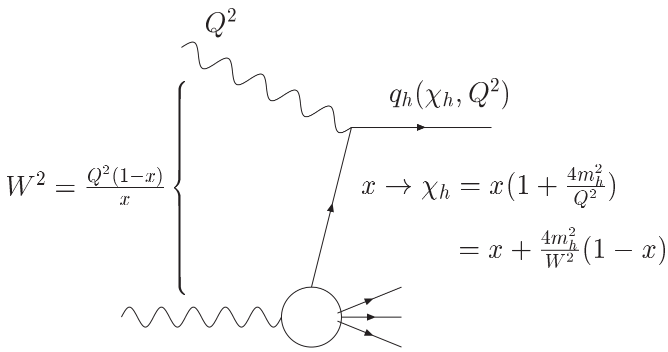

Figure 8.1: Introduction of the χ_h parameter in the $\mathrm{DIS}_{e\gamma}$ scattering.

where we used the $W^2 = Q^2(1-x)/x$ relation. Still, that is not the most general form of the χ_h variable. The $W > 2m_h$ condition has to be applied in the case of the processes where only one photon interacts via the heavy quark. Let us stress that the second heavy quark, or more precisely its anti-quark, propagates among the remnants of the photon. Therefore, the expression (8.6) seems to be adequate for the DR parton processes such as $\gamma + h^\gamma \to G + h$ and the RR process such as $G^\gamma + h^\gamma \to G + h$. In the case of the double-resolved photon processes with two heavy quarks interacting, as in the $h^\gamma + \bar{h}^\gamma \to h + \bar{h}$ process, the number of the produced heavy quarks equals four (two of them among photon remnants). Hence the appropriate χ_h formula reads then

$$\chi_h = x + \frac{16m_h^2}{W^2}(1-x), \tag{8.7}$$

which fulfills the $\chi \to 1$ for $W \to 4m_h$ condition.

We conclude that the general form of the χ_h variable which should be used in the computation of the heavy-quark densities in the photons, in any process where n heavy-quark pairs are produced (with half of the heavy quarks among the photon remnants) is

$$\chi_h(n, W^2) = x + n^2\frac{4m_h^2}{W^2}(1-x). \tag{8.8}$$

In such case, still the transverse momentum of the produced heavy quark may be used as the hard scale in parton densities. That means that two distinct energy scales are necessary in calculation of the q_h^γ density in the ACOT(χ) scheme. We can write it as $q_h^\gamma(\chi_h(n, W^2), p_T^2)$ or most generally as $q_h^\gamma(\chi_h(n, W^2), \mu^2)$.

In the $\mathrm{DIS}_{e\gamma}$ scattering $n = 1, \mu^2 = Q^2$ and $W^2 = Q^2(1-x)/x$ leading to the $q_h^\gamma(x, Q^2) \equiv q_h^\gamma(\chi_h(x, Q^2), Q^2)$ parametrizations given in all our analyses, [60, 61, 64, 102].

The procedure of the introduction of the χ_h variables in the $\mathrm{DIS}_{e\gamma}$ scattering and the $\gamma\gamma$ interaction is illustrated in Figs. 8.2 and 8.2, respectively.

The proposed approach to the calculation of the heavy-quark contributions to resolved-photon processes requires the process dependent $\chi_h(n, W^2)$ variables and parametrizations of

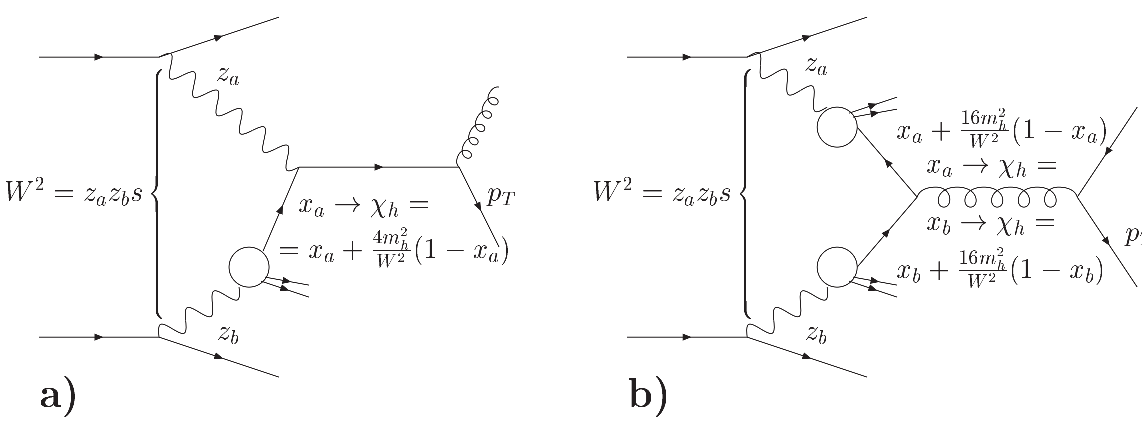

Figure 8.2: Introduction of the χ_h variables in the $e^+e^- \to e^+e^- + h/\bar{h} + X$ process, a) the single resolved-photon (DR) and b) the double resolved-photon (RR) process.

the heavy-quark densities in form of the functions of χ_h, $q_h^\gamma(\chi_h(n, W^2), Q^2)$ (see also Appendix C and the web-page [99]). For the single resolved-photon process we find then

$$\begin{aligned} \sigma(e^+e^- \to e^+e^- + h/\bar{h} + X)|_{\mathrm{DR}} &= \int_0^1 dz_a \int_0^1 dz_b \; f_{\gamma/e}(z_a) f_{\gamma/e}(z_b) \\ & \int_0^1 dx_b \; f_j^\gamma(\chi_{h,b}(1, W^2), \mu^2) \; \hat{\sigma}(ij \to h/\bar{h} + X), \quad (8.9) \end{aligned}$$

where $\chi_{h,b}$ corresponds to x_b, and a similar expression for the RR processes (with $n = 1$ or 2).

Let us now compare the results of the computation of the LO cross-sections for the charm- and beauty-quark $e^+e^- \to e^+e^- + h/\bar{h} + X$ production performed in various schemes as a function of the total e^+e^- system energy $\sqrt{s} = 2E_{\mathrm{beam}}$ with the data obtained in [104–114] including the recent preliminary DELPHI measurement of the beauty-quark production cross-section (results of experiments [104–110] were extrapolated to the total charm cross-sections in [115]). The comparison is shown in three plots, Figs. 8.3-8.5, with different ACOT(χ) type predictions. In all plots we present the same FFNS scheme predictions obtained with the use of the GRS LO [6] (with $m_c = 1.4$ GeV and $m_b = 4.5$ GeV) and FFNS$_{CJK}$2 LO parametrizations, and for comparison the direct $\gamma\gamma \to h + \bar{h}$ contribution. The ACOT1(χ) denotes the approach with the use of the q_h^γ densities using the old form of the χ_h variable for the DIS$_{e\gamma}$ scattering, given by Eq. (8.2), while in the ACOT2(χ) scheme the general $q_h^\gamma(\chi_h(n, W^2), Q^2)$ parametrization was applied. In Fig. 8.3 'massless' ACOT1 & 2(χ) schemes were used with the $p_T > 2$ GeV ($p_T > 5$ GeV) condition, applied in the computation of the massless parton cross-sections containing charm (beauty) quarks in the initial state. In Fig. 8.4 again 'massless' ACOT(χ) schemes were used but no p_T constraint was applied. In order to suppress large contributions at low values of the transverse momentum, the massless parton cross-sections have been multiplied by $G(m_h, p_T^2)$ introduced in [11, 72] as

$$G(m_h, p_T^2) = \frac{p_T^2}{p_T^2 + c^2 m_h^2}, \quad (8.10)$$

with $c = 5$. Finally in Fig. 8.5 'massive' ACOT1(χ) and ACOT2(χ) schemes were used.

As can be seen in the plots, in each case the ACOT2(χ) approach gives best description of the $\gamma\gamma$ heavy-quark production data. Moreover the 'massive' ACOT2(χ) scheme, the only one in which we do not suppress the cross-section at small p_T in an arbitrary way, produces the bottom-quark cross-section which differs from the experimental results measured by the L3 and OPAL collaborations by only one standard deviation. Still, in this approach we obtain the charm-quark production cross-section lying slightly above most of the data points for $\sqrt{s} \geq 70$ GeV and in addition we have to keep in mind that the existing NLO calculations for that process lead usually to higher cross-sections than the LO ones. On the other hand we apply low value of the charm-quark mass ($m_c = 1.3$ GeV) and the cross-section for its production is very sensitive to the change of this parameter. Generally, the higher m_h the lower $\sigma(e^+e^- \to e^+e^- + h/\bar{h} + X)$. Contrary to the results obtained in the ACOT2(χ) approach the ACOT1(χ) scheme gives very similar cross-sections in both 'massless' and the 'massive' calculations for both, charm and beauty quark. These results are close to the cross-sections computed in the FFNS scheme in which we applied our FFNS$_{CJK}$2 LO parton parametrization. On contrary the FFNS scheme with the GRS LO parametrization predicts much lower cross-sections, in the charm-quark production close to the direct contribution. The reason is twofold. Firstly, it is caused by the differences among the FFNS$_{CJK}$ LO and GRS LO parton densities and secondly by the differences among the values of the heavy-quark masses applied in both parametrizations and the analysed calculations.

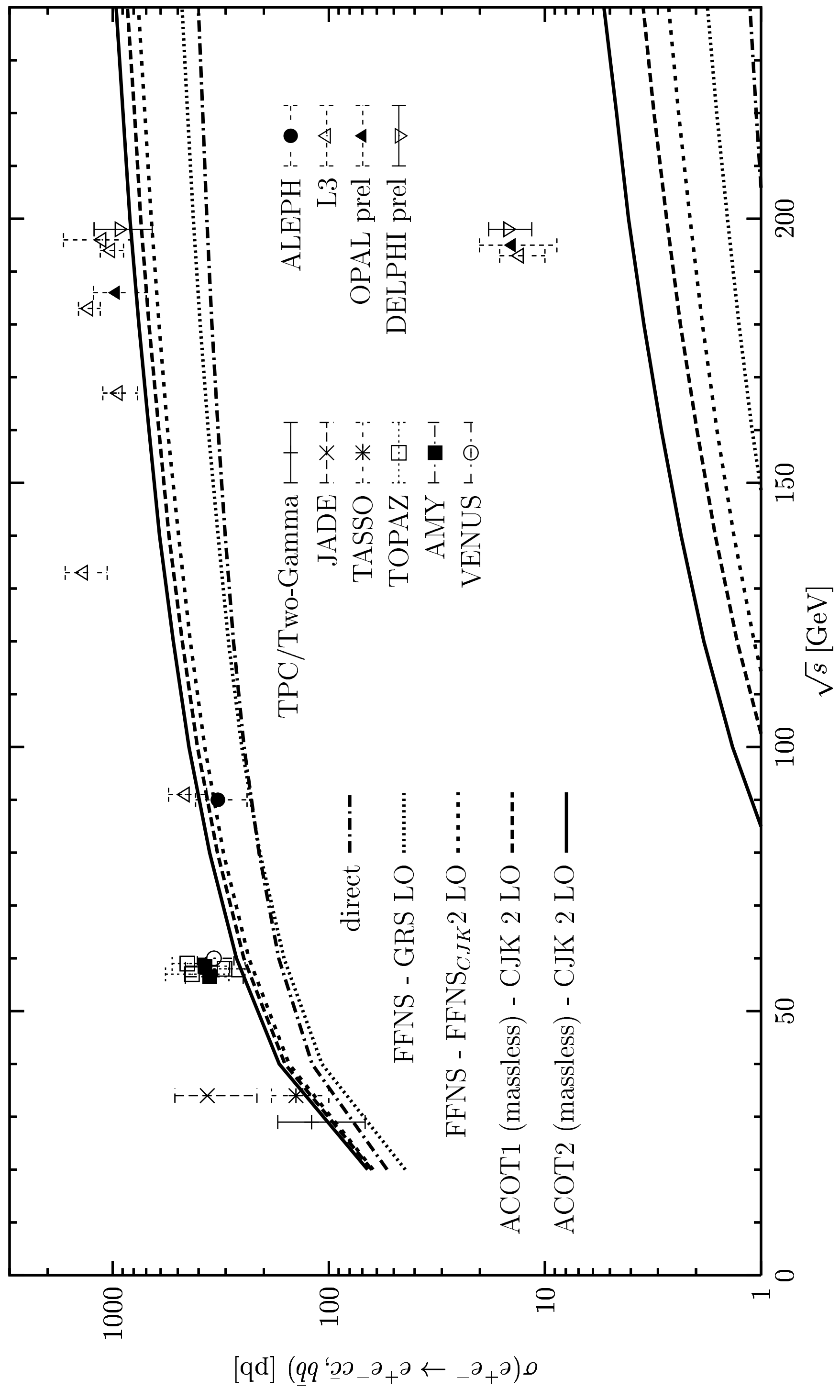

Figure 8.3: Comparison of the LO charm- and beauty-quark $e^+e^- \to e^+e^- + h/\bar{h} + X$ production cross-sections as the function of the square of the total e^+e^- system energy $\sqrt{s} = 2E_{\mathrm{beam}}$ calculated in the FFNS scheme and in two different 'massless' ACOT(χ) approaches described in the text. In the FFNS scheme we use the GRS LO [6] and FFNS$_{CJK}$2 LO parametrizations. In the ACOT(χ) approaches the CJK 2 LO parametrization is applied and the transverse momentum of the produced heavy-quark is constraint to $p_T > 2$ GeV and $p_T > 5$ GeV in the charm- and beauty-quark case, respectively. In addition the direct (DD) $\gamma\gamma \to h\bar{h}$ contribution to the process is shown. The data points were obtained in [104–112]. Results of experiments [104–110] were extrapolated to the total charm cross-sections in [115].

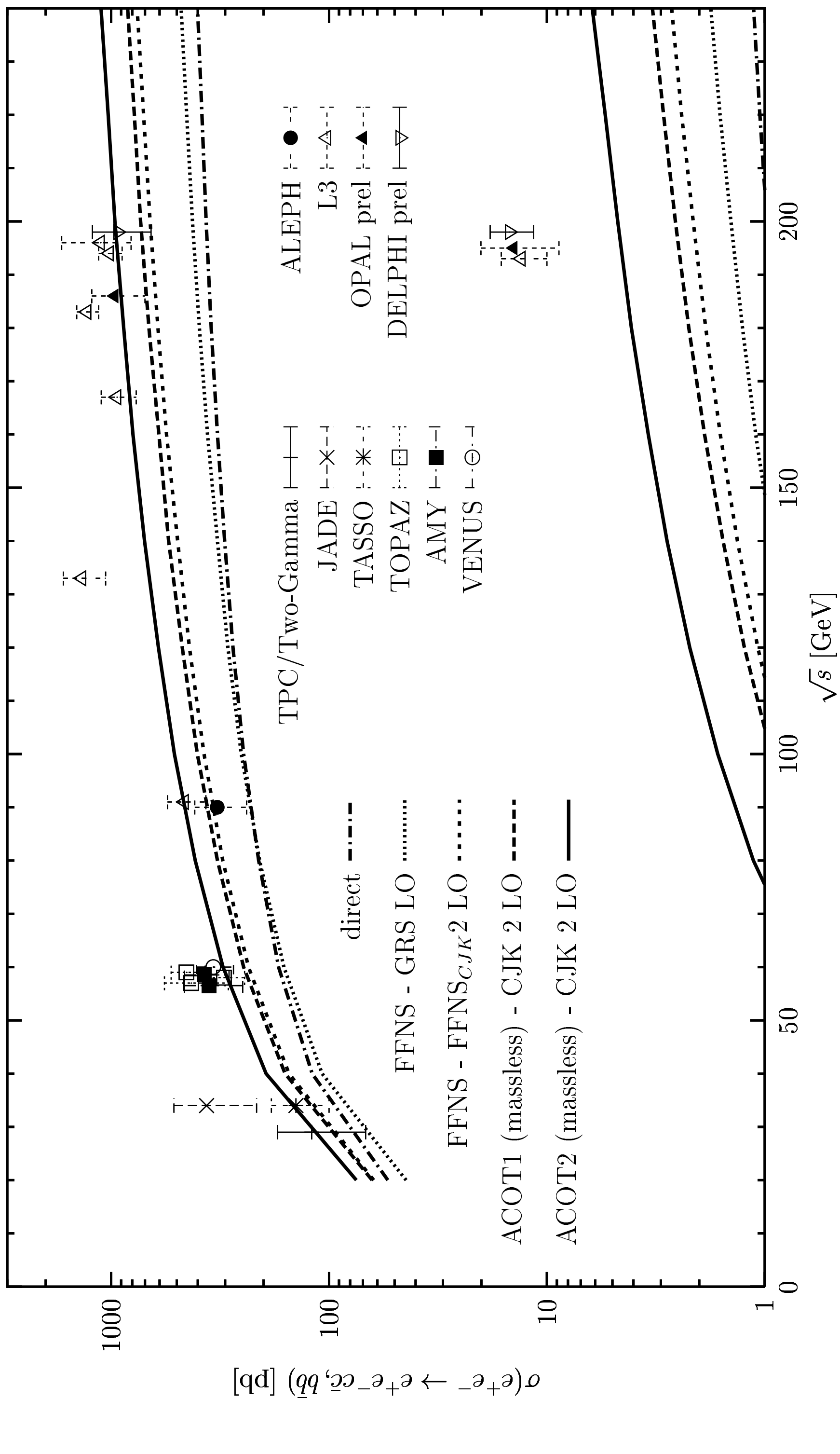

Figure 8.4: Same as in Fig. 8.3 but here the massless parton cross-sections multiplied by $G(m_h, p_T^2) = p_T^2/(p_T^2 + c^2 m_h^2)$, with $c = 5$, were used in ACOT(χ) predictions.

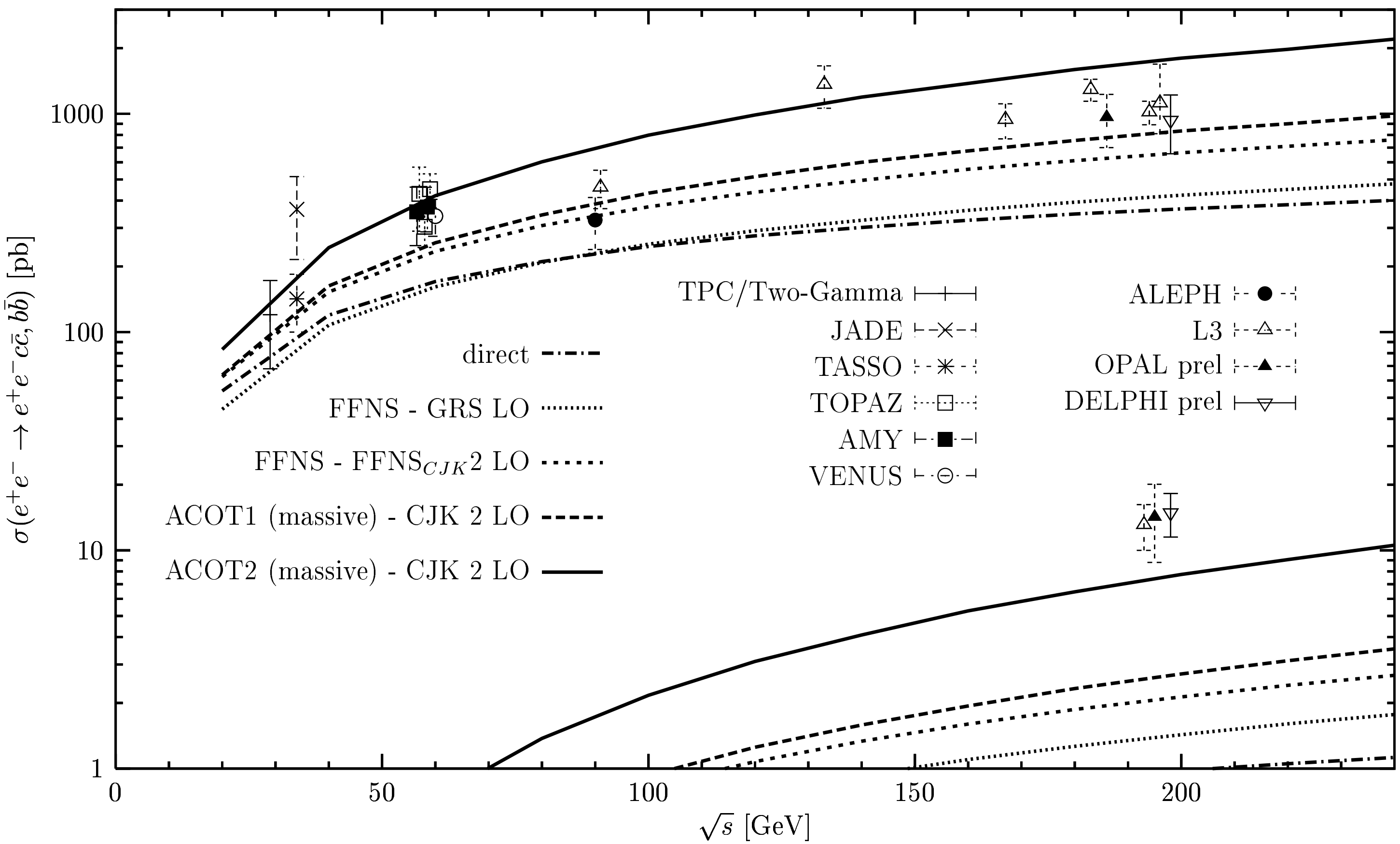

Figure 8.5: Same as in Fig. 8.3 but the 'massive' ACOT(χ) approaches were used.